ICSO 2016

International Conference on Space Optics

Biarritz, France

18–21 October 2016

Edited by Bruno Cugny, Nikos Karafolas and Zoran Sodnik

Backside illuminated CMOS-TDI line scanner for space applications

O. Cohen

N. Ben-Ari

I. Nevo

N. Shiloah

et al.

BACKSIDE ILLUMINATED CMOS-TDI LINE SCANNER FOR SPACE APPLICATIONS

O. Cohen, N. Ben-Ari, I. Nevo, N. Shiloah, G. Zohar, E. Kahanov, M. Brumer, G. Gershon, O. Ofer
SemiConductor Devices (SCD) P.O.B. 2250, Haifa, 3102102, Israel, omerc@scd.co.il

ABSTRACT

A new multi-spectral line scanner CMOS image sensor is reported. The backside illuminated (BSI) image sensor was designed for continuous scanning Low Earth Orbit (LEO) space applications including A custom high quality CMOS Active Pixels, Time Delayed Integration (TDI) mechanism that increases the SNR, 2-phase exposure mechanism that increases the dynamic Modulation Transfer Function (MTF), very low power internal Analog to Digital Converters (ADC) with resolution of 12 bit per pixel and on chip controller. The sensor has 4 independent arrays of pixels where each array is arranged in 2600 TDI columns with controllable TDI depth from 8 up to 64 TDI levels. A multispectral optical filter with specific spectral response per array is assembled at the package level. In this paper we briefly describe the sensor design and present some electrical and electro-optical recent measurements of the first prototypes including high Quantum Efficiency (QE), high MTF, wide range selectable Full Well Capacity (FWC), excellent linearity of approximately 1.3% in a signal range of 5-85% and approximately 1.75% in a signal range of 2-95% out of the signal span, readout noise of approximately 95 electrons with 64 TDI levels, negligible dark current and power consumption of less than 1.5W total for 4 bands sensor at all operation conditions .

INTRODUCTION

A new multi-spectral, BSI, all CMOS technology, TDI, Radiation Hardened (RadHard), line scanner sensor has been designed for continuous scanning LEO space applications, as an upgrade for Charged Coupled Devices (CCD's). The sensor design stage is complete and some prototypes have been manufactured (shown in **Fig. 1**) and characterized. In this article we briefly describe the sensor design, architecture and recent measurements that were performed. Important characteristics of the sensor are presented, including QE, static MTF and linearity.

SENSOR DESIGN

The fundamental functionality of the CMOS TDI sensor is to transduce the incoming light signal into an electrical signal. In the current sensor, the transduction is made by a well-known CMOS Four Transistor (4T) Active Pixel Sensor (APS) architecture [1], [2], and [3]. A state of the art custom 4T pixel was designed to fit the required sensor's parameters such as conversion gain and readout speed. However the functionality of the custom pixel is equivalent to other common 4T devices.

The line scanning CMOS TDI sensor outputs a line of 2,600 pixels per image cycle, where the other dimension of the image is acquired by the scanning operation of the LEO satellite. When a high scanning throughput is required only a short exposure period is available which results in a low signal. Thus, in order to improve the Signal to Noise Ratio (SNR) a TDI arrangement was implemented. The TDI design includes several pixels arranged along the scanning direction where each of these pixels collects photons from the same part of the scene at a different instant in time. The signal is then integrated with the appropriate time delay, allowing higher signal and improved SNR. The TDI format in the sensor allows registration of the same part of the scene up to 64 times. Hence, the sensor has an array of 2,600 pixels by 64 TDI levels. The acquisition of the image is done by an electronically controlled rolling shutter. The shutter is controlled by communication commands which enable the exposure time to be changed from the line time down to zero exposure in steps of 1/1024.

The sensor internal configuration is designed for two phase exposure described in [4] where the first and second halves of the exposure are half pixel shifted in a synchronized manner with the scanning motion. As a result of the two phase exposure the dynamic MTF of the image captured by the moving rectangular pixels is improved from 63% to 91% without sacrificing any other performance parameter. The whole process of two phase exposure, signal collection and TDI operation is synchronized and controlled by an internal self-sustained controller.

The photon signal is converted to voltage by the pixels, and it is then digitized by an internal Analog to Digital Converter (ADC). The signal out of a single pixel is converted at low resolution and by integration of the 64 TDI levels the depth of sampling is increased to 12bits.

Fig. 1. BSI CMOS TDI line scanner image sensor prototype

A Read Out Channel (ROC) is defined as the medium connecting a pixel to a video output channel. One ROC contains a unique combination of a 2 phase exposure mechanism, ADC and TDI mechanism. A single band contains approximately 170,000 different ROCs. The internal controller mentioned above is responsible for the control of the whole ROC operation and synchronization.

A single sensor contains 4 bands. Each band includes an array of 2,600 pixels by 64 TDI levels, all the ROC's, a self-sustained internal controller, a communication controller, a video output port and all the necessary peripheral support blocks. At the silicon chip level, each band is an autonomous sensor sharing only the silicon bulk with the other 3 bands and differs from the other 3 bands only by a communication address. The sensor architecture is described in block diagram form for a single band in **Fig. 2**.

Each of the 4 bands can have a specific optical filter. The optical filter has an optical coating with a narrow transmission band deposited over a glass substrate which is accurately mounted on the ceramic package 0.5mm above the silicon chip. Any selection and arrangement of filters is possible as required by the application.

The sensor's ceramic package provides a highly accurate mounting surface as well as an electrical interface. The package can be sealed with adhesives. The electrical interface is provided by two connectors. In order to reduce the number of pins of the sensor, some signals which are common to all 4 bands such as power supplies and clocks are shared at the package level.

The main features and designed performance are summarized in **Table 1**.

Table 1. Features and designed performance

Parameter	Value
Detector type	VIS-NIR CMOS TDI line scanner
Spectral bands	4, customer selectable bands (400nm-900nm)
Format	4 independent lines, 2600 pix each
Pitch	26μm
TDI depth	8 up to 64 (in steps of 8)
Pixel capacity	>300Ke-
Floor noise	<80e-
Dynamic range	72dB
Linearity	<2% (5% up to 85% of full scale)
Maximum line rate	10,000 line/sec
Power dissipation	<2W (@max line rate)
Power supplies	3.5V, 1.8V, reference 2.5V
Video output	Digital, 12bit
Communication	Serial port
Clocks	Main: single LVDS up to 58MHz, line sync
Readout direction	Bi-directional
Environment	RadHard, Space applications
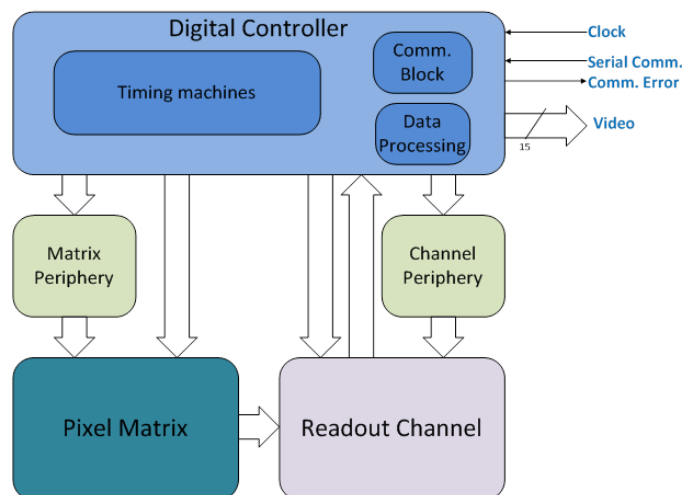
Fig. 2. Single band block diagram

MEASUREMENTS AND PERFORMANCE

A. Setup

The measurement setup includes a quartz halogen light source coupled to a filter wheel and an integration sphere, a parametric tester and interfacing mechanical and electrical adapters. The filter wheel has 8 positions, 7 incorporate narrow band filters (approximately 30 nm full width half maximum) and one is clear. The central transmission wavelengths of the filters are 438, 488, 579, 681, 780, 880 and 935 nanometres. The integration sphere output intensity is calibrated for each filter including the open slot. The calibrated integration sphere ensures uniform and controlled light intensity. The mechanical adapters position the sensor in front of the integration sphere orifice. The distance between the sensor and the integration sphere output port defines the optical F-number. In most of the measurements the sensor was positioned at a distance equivalent to F/1. The tested CMOS sensor unit requires supply of power, clock and a few control signals. All of these are supplied by the parametric tester. The same tester acquires the output of the sensor including the digital image data and some control signals. The output of the sensor is converted to a binary file and analysed using MATLAB.

B. Full Well Capacity

The Full Well Capacity (FWC) defines the saturation level of the sensor in terms of electrical charge which in an ideal sensor is generated only by the photons signal. In general the saturation of a digital CMOS sensor may occur due to one or more limiting effects. In the CMOS TDI sensor reported here the FWC is limited by the ADC span. The ADC span is controlled electronically. Therefore it is possible to tune the FWC to different values. Fig. 3 shows the distribution of several sensors calibrated to a FWC of 280Ke-. One of the sensors was tuned to a FWC of between 250Ke- and 350Ke-. However, the design enables a wider span of calibration, estimated to be between 100Ke- and 400Ke-.

C. Linearity

The deviation from linearity of the sensor is defined as the peak to peak deviation from a best fit linear regression of the signal vs. the Total Illumination Energy (TIE). Changing the sensor's electronic shutter duty cycle or exposure ratio (defined as: shutter duty cycle×1,024) is equivalent to a change in the TIE and is sometimes presented as such. Various effects degrade the linearity of the sensor at either end of the signal span. Hence, it is conventional to define the linearity within a range covering most but not all of the signal span. We define the linearity in two ranges, 5-85% and 2-95% out of the signal span. As described above each band has approx. 170,000 ROC's. The signal vs. TIE is measured for each ROC and the peak to peak error is extracted from a linear fit of each ROC's response. Excluding a minute number of null functioning ROC's the worst peak to peak error is defined as the result for each band. The results shown in **Table 2** are the average and standard deviation of linearity of a population of bands in the two ranges defined above.
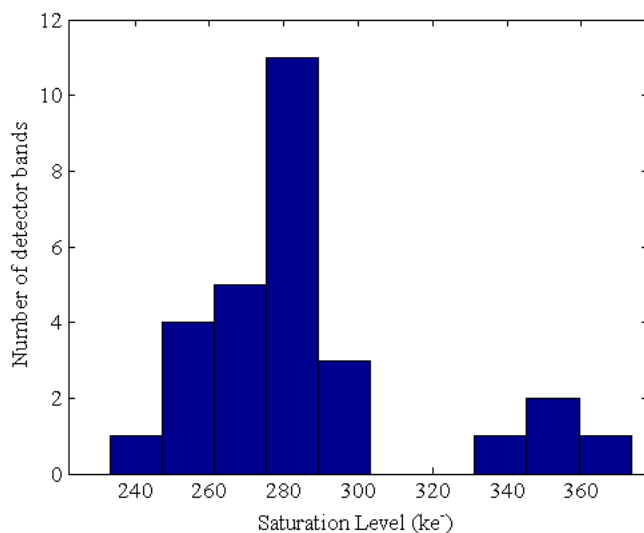
Fig. 3. Distribution of full well capacity among population of sensors

Table 2: Average linearity

Linearity range	Measured Value
5-85%	1.3%±0.2%
2-95%	1.75%±0.3%
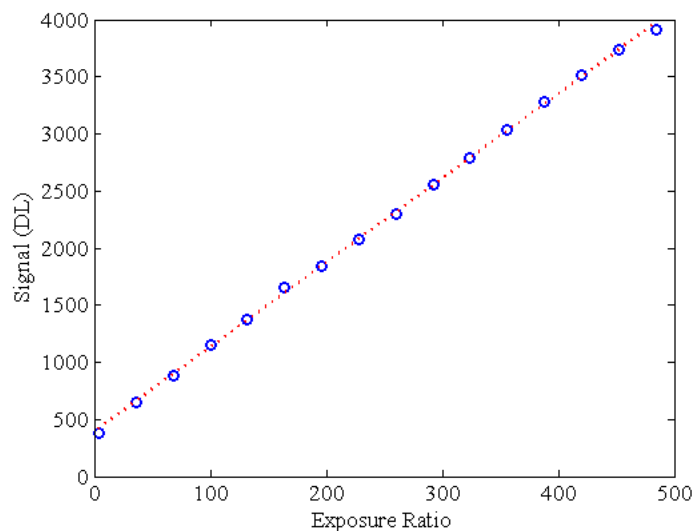
Fig. 4. Signal in digital levels vs. the exposure ratio (The exposure time is linearly dependent on the exposure ratio and 1024 corresponds to the maximum exposure time at a specific line rate). The luminance is 0.1 Watt/centimeter^2/steradian with 488nm narrow band filter.

The graph in **Fig. 4** shows the linear response of the sensor demonstrating the median of the output of all ROCs at a specific signal level vs. the exposure ratio. The slope of the graph depends on the illumination intensity (TIE). In **Fig. 4** a constant illumination intensity is selected to ensure that the full signal span is achieved below an exposure ratio of 500. The measured linearity is well within the requirements in **Table 1**.

Table 3. Measured readout noise over population of sensors.

Readout Noise	Value
Measured in e-	95±15
Measured in DL	1.2±0.2
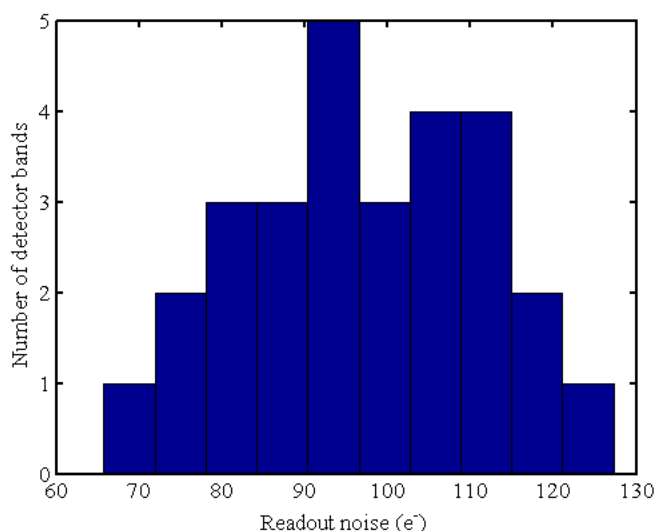
Fig. 5. Distribution of readout noise among the sensor population
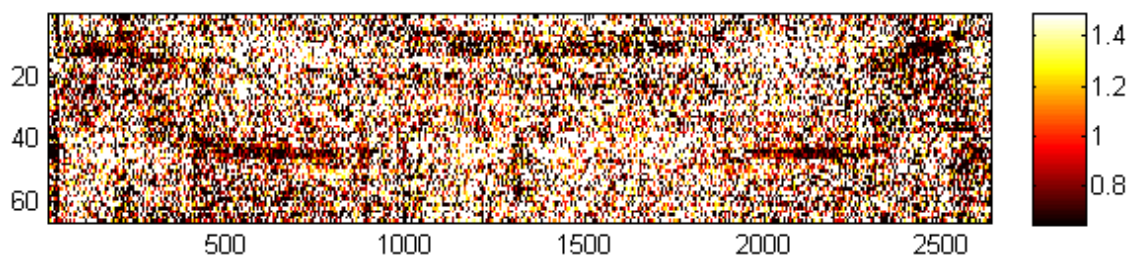
Fig. 6. Spatial distribution of readout noise in a single band showing all the ROC (color map is in DL).

D. Readout Noise

The readout noise of the sensor was measured by two methods. One method used a Photon Transfer Curve and the readout noise was extracted as the intercept of the Photon Transfer Curve with the squared noise axis. **Table 3** shows the average measured readout noise of a population of sensors and the standard deviation using this method of measurement. The readout noise is expressed in terms of charge (e-) or Digital Level (DL). The distribution of the measurements in terms of charge (e-) is shown in **Fig. 5**.

In the second method the pixels were turned off and the signal out of the ROCs was measured. The results are shown in **Fig. 6** mapping all the ROCs of a single band and showing the spatial distribution within the band. The results in both methods are identical up to the accuracy of the measurement.

E. Power Consumption

The sensor power consumption is dependent on several parameters (e.g. line rate). The measurement setup defines the load on the video outputs of the sensor and thus the output drives power consumption. The current setup load is significantly higher than the 20 pF specified load on each video output signal. As a result, a measurement that includes the output signal drivers is biased. To avoid bias by the over load of the output signals we measured the power consumption of the sensor without the output drivers, as shown in **Fig. 7.** To estimate the additional power consumption by the output drivers, one can use the following equation:

$$P_{video\_output} \cong 2.6(\mu W \times \sec) \times L_{rate} \times B \tag{1}$$
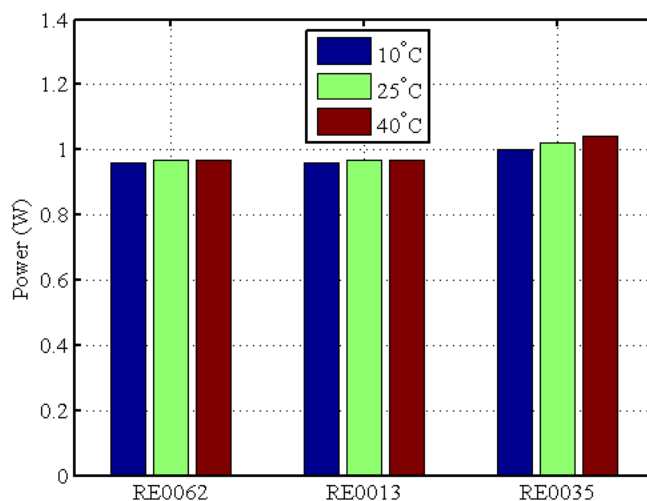
Fig. 7. Power consumption of 3 sensors (RE0062, RE0013, RE0035) at 7,500 lines per second - total of 4 bands per sensor, not including the video outpout. Measured at 3 sensor temperatures.

where L_{rate} is the line rate in units of *lines/sec* and *B* is the number of bits (12 bits max.) switched from pixel to pixel. At a line rate of 7,500 lines per second and switching all 12 bits the power consumption of the output drivers is 234mW. The calculated video output driver power consumption should be added to the measured power. The total power consumption including the output drivers is well below the requirement defined in **Table 1**.

F. Quantum Efficiency

Two types of sensor were manufactured: a thin absorbing layer sensor which is more suitable for the blue spectrum and a thick absorbing layer sensor which is more suitable for the red and near infrared spectrum. Both types of sensor are BSI. A simple model of absorption in silicon is suggested for both types of sensor. The model assumes perpendicular light incidence and includes the transmission of the Anti-Reflective Coating (ARC), the absorption of the silicon layer, partial reflection from the electronic circuit underneath the silicon, second absorption by the silicon layer and exit of the light. This model does not include surface effects of the silicon which are dominant in the UV and blue spectrum due to the very short absorption length. Hence, the model is inaccurate below 600 nm. The expected external QE based on the model described above and the results of measurements of both types of sensor are shown in **Fig. 8**. There is good agreement between the model and the measurements above 600 nm. The measurement results do not take into account a filter or a window coating. A practical device would include a window with or without a filter and the transmission of this element should also be taken into account. The sensor BSI structure absorbs light that is incident of any area above the absorbing layer. Hence, the fill factor is considered 100%.

G. MTF

The static MTF measurement setup includes a Knife Edge Target and several Resolution Targets. The Knife Edge measurement technique is less susceptible to DC errors and therefore the results are more accurate. The measurement results of the Knife Edge technique for both the thin absorption layer and the thick absorption layer sensors are shown in **Fig. 9**. The Resolution Target measurements were slightly higher but assumed to be less accurate and therefore are not shown here. The MTF of the thin layer sensor is expected to be higher at the blue end of the spectrum and lower at the NIR end, compared to the thick layer sensor. The measurement results are in good agreement with the expected performance.
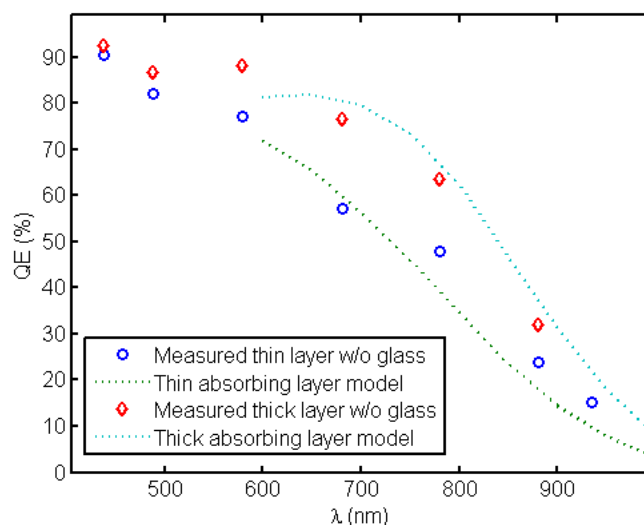
Fig. 8. Measured Quantum Efficiency of the thin and thick absorption layer sensors (circles and diamonds points respectively) and simulation for thin and thick absorption layers (dashed lines).
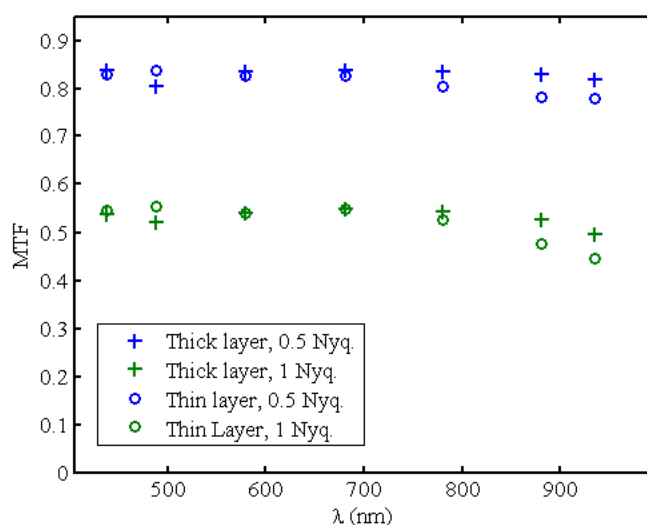
Fig. 9. Spectral Modulation Transfer Function measured with the thick absorption layer sensor (plus points) and the thin absorption layer sensor (circle points) at Nyquist (green) and half Nyquist (blue) frequencies.

H. Dark Current

The dark current is linearly dependent on the exposure time. **Fig. 10** shows the linear dependence of the signal measured without illumination in a dark chamber. The dark current is extracted from the slope. In order to observe the dark current, long exposure times are required, which are only achievable at very low line rates. For the thick absorption layer sensor the dark current measured at room temperature is approximately 70,000 electrons/sec/pixel (counting all 64 TDI levels) thus contributes a signal equivalent to less than 9 DL at 100 lines per second and full exposure time. In terms of noise the contribution of the dark current is equivalent to approximately 26 electrons, a negligible number compared to the readout noise. For the thin absorption layer sensor the dark current measured at room temperature is approximately 11,000 electrons/sec/pixel (counting all 64 TDI levels) which contributes a signal equivalent approximately 1 DL at 100 lines per second and full exposure time. The dark current is therefore insignificant.
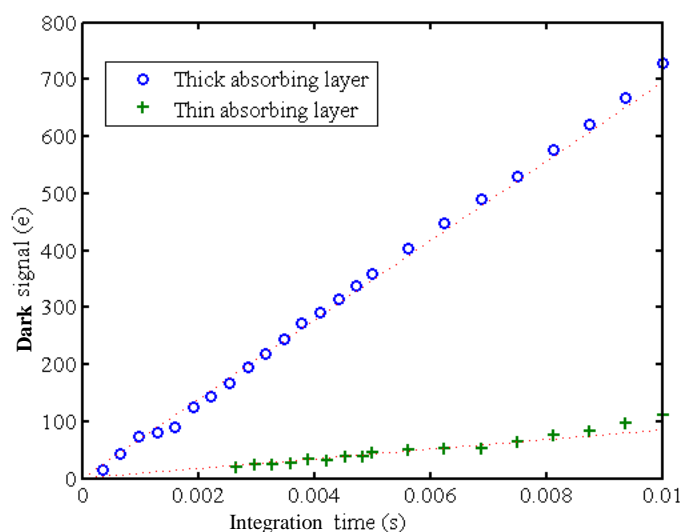
Fig. 10. Dark signal (in e-) vs. integration time of thick absorption layer sensors (blue cilrcles), and of thin absorption layer sensor (green plus), measured at 100Hz line rate allowing maximum integration time of 0.01 seconds. The dotted lines represent linear fits to the data (with zero offset).

CONCLUSIONS

A very high performance CMOS TDI line scanner sensor was designed and manufactured. Among the CMOS-TDI sensor advantages are the high level of integration including on-chip ADC, on-chip controller, and CMOS compatible voltage levels, thus reducing the power consumption and the weight of the supporting electronics as well as providing a simple interface. The major performance parameters have been characterized and are reported in this paper. The results show good agreement with the expected values for QE and MTF. The FWC is selectable within a wide range including the required 300,000 e-. The sensor has excellent linearity of approximately 1.3% in a signal range of 5-85% and approximately 1.75% in a signal range of 2-95% out of the signal span. The readout noise of approximately 95 electrons with 64 TDI levels is about 20% higher than expected but still enables very high performance. The dark current contribution to the signal and to the noise is negligible. The power consumption of less than 1.5W total for 4 bands sensor at all operation conditions is well below the required value. Further measurements and tests will be performed to complete the sensor characterization.

ACKNOWLEDGEMENT

REFERENCES

[1] E. R. Fossum, D. B. Hondongwa, "A Review of the Pinned Photodiode for CCD and CMOS Image Sensors", IEEE Journal of The Electron Devices Society, Vol. 2, No. 3, May 2014, pp. 33- 43.
[2] R. Coath, J. Crooks, A. Godbeer, M. Wilson, R. Turchetta,, " Advanced Pixel Architectures for Scientific Image Sensors", in Proc.Topical Workshop Electronics for Particle Physics, Paris, France, Sep.21–25, 2009, pp. 57-61
[3] R. Guidash, T. Lee, P. Lee, D. Sackett, C. Drowley, M. Swenson, L. Arbaugh, R. Hollstein, F. Shapiro, S. Domer, "A 0.6 m CMOSpinned photodiode color imager technology," in Proc. Technical Digest IEEE Electron Device Meeting,Washington, DC, Dec. 7–10, 1997, pp. 927–929.
[4] Kodak CCD Primer, #KCP-001, "Charge-Coupled Device (CCD) Image Sensor", Eastman Kodak Co., Microelectronics Technology Div., Rochester, NY. www.kodak.com.